

## A STUDY OF SPIN REORIENTATION IN $\text{NdFe}_{12-x}\text{V}_x$ BY MÖSSBAUER AND MAGNETIZATION MEASUREMENTS

C. CHRISTIDES, A. KOSTIKAS, A. SIMOPOULOS, D. NIARCHOS and G. ZOUGANELIS

*National Center for Scientific Research "Demokritos", Institute of Materials Science, 153 10 Ag. Paraskevi Attiki, Greece*

Received 31 July 1989; in revised form 2 October 1989

The spin reorientation transitions in the intermetallic compounds  $\text{NdFe}_{12-x}\text{V}_x$  ( $x = 2.2, 2, 1.8$ ), which crystallize in the tetragonal  $\text{ThMn}_{12}$  structure, have been studied by Mössbauer and magnetization measurements on oriented absorbers. The spin reorientation has its onset in the range of 110–130 K and is completed in a few kelvin. The Mössbauer spectra have been analyzed with a model which takes into account the preferential occupation by V of the i-sites in the  $\text{ThMn}_{12}$  structure. The temperature dependence of the canting angle has been determined both by this analysis and from the magnetization data.

### 1. Introduction

Spin reorientation phenomena are observed in rare earth–iron alloys as a result of the variation with temperature of competing anisotropies between the iron and rare earth sublattices. These interactions, in combination with magnetic exchange, determine the orientation of the saturation magnetization with respect to the crystallographic axes.

The anisotropy energy of the rare earth sublattice in a crystal with tetragonal symmetry is given by the phenomenological expression

$$E_R = K_1 \sin^2\theta + (K_2 + K'_2 \cos 4\varphi) \sin^4\theta + (K_3 + K'_3 \cos 4\varphi) \sin^6\theta, \quad (1)$$

where the constants  $K_i$ ,  $K'_i$  are related to the crystal field parameters  $B_{nm}$  for the rare-earth-ion site. The iron sublattice anisotropy is usually represented by the first-order term where the constant  $K(\text{Fe})$  is determined by measurements on compounds with  $R = \text{Y, Gd or Lu}$ .

The pseudobinary compounds with the general formula  $\text{RFe}_{12-x}\text{T}_x$ , which are possible candidates as permanent magnet materials, crystallize in the tetragonal  $\text{ThMn}_{12}$  structure. Spin reorientation transitions have been reported in these compounds with  $T = \text{Ti}$  and  $R = \text{Nd, Tb, Dy, Er}$  [1,2].

We have also recently reported preliminary measurements on  $\text{NdFe}_{9.8}\text{V}_{2.2}$ , which indicate the occurrence of a spin reorientation transition [3]. In the alloys of this group the iron sublattice anisotropy favors orientation along the  $c$ -axis, as determined from magnetic measurements on the members with  $R = \text{Y, Gd, Lu}$ . Using a crystal field model for the anisotropy of the crystal lattice, Hu et al. [2] have calculated the crystal field parameters  $B_{nm}$ , from the variation with temperature of the angle between the direction of the moment and the  $c$ -axis. A similar model has been applied previously for the calculations of the canting angle in  $\text{Nd}_2\text{Fe}_{14}\text{B}$  [5].

The angle  $\alpha$  of the magnetic moment with respect to the  $c$ -axis can be determined as a function of temperature by Mössbauer measurements on oriented absorbers from the variation of the relative intensity of the  $\Delta m = 0$  lines. Magnetization measurements on oriented absorbers can also be used for the same purpose. We report in this paper detailed magnetization and Mössbauer measurements on samples of  $\text{NdFe}_{12-x}\text{V}_x$  ( $x = 1.8, 2.0, 2.2$ ) alloys from which the variation of the angle  $\alpha$  with temperature is deduced.

A major problem in extracting the angle  $\alpha$  from Mössbauer or magnetization data on oriented absorbers is the incomplete alignment of crystallites during the preparation of oriented absorbers in an

epoxy matrix under a high magnetic field. The misalignment is most pronounced in those cases, as that examined here, where the opposite signs of anisotropy constants  $K_1$  for Nd and  $K_1(\text{Fe})$  lead to a small anisotropy field  $B_A < 2$  T. For a correct determination of the angle, the distribution of orientation of crystallites must be properly taken into account. We have used for this purpose methods of analysis introduced earlier for similar problems by Serle et al. [6] and Hu et al. [1].

An additional complication in the analysis of Mössbauer spectra is the distribution of nonmagnetic atoms (V in our case) in the different iron sites, which leads to a variation of hyperfine parameters and hence an increase in number of free parameters necessary for fits of spectra. A significant reduction in the number of free parameters can be achieved by using a model of occupation probabilities of the different sites. This has been used previously for the analysis of Mössbauer spectra of  $\text{RFe}_4\text{B}$  compounds [7].

## 2. Experimental details and X-ray analysis

Samples with nominal composition  $\text{RFe}_{12-x}\text{V}_x$  ( $x = 1.8, 2, 2.2$ ) were prepared from 99.99% pure starting materials. After arc melting, the samples were sealed into evacuated quartz tubes and annealed at  $850^\circ\text{C}$  for two weeks. X-ray diffraction was performed on powder samples with a Philips X-ray powder diffractometer using  $\text{Co-K}\alpha$  radiation.

The X-ray diagrams of the annealed  $\text{NdFe}_{12-x}\text{V}_x$  alloys were indexed on the basis of the tetragonal  $\text{ThMn}_{12}$  type structure. A small fraction of Fe-V was observed in the  $\text{NdFe}_{10.2}\text{V}_{1.8}$  sample. The other two samples with  $x = 2.2, 2$  were of the single-phase  $\text{ThMn}_{12}$  type structure. Unfortunately, theoretical calculations for the intensities of X-ray data cannot give us any information for the distribution of V over the three inequivalent crystallographic sites 8i, 8f and 8j, because the difference in atomic scattering factors between Fe and V atoms is small. Neutron diffraction performed on  $\text{YFe}_{10}\text{V}_2$  [8] has shown that there is a preferential occupation of V for the 8i site, which was explained in terms of enthalpy effects [9]. We

Table 1

Lattice constants, Curie temperatures  $T_c$  and saturation magnetization  $M_s$  for  $\text{NdFe}_{12-x}\text{V}_x$  compounds as a function of V concentration  $x$

$x$	$a$ (nm)	$c$ (nm)	$T_c$ (K)	$M_s$ ( $\mu_B/\text{f.u.}$ )	
				R.T.	L.He
1.8	0.85	0.47	630	18.2	20.7
2.0	0.85	0.47	605	17.2	18.4
2.2	0.85	0.47	580	15.7	17.6

assume then that this preference of V atoms must be valid for our sample also. The lattice constants, determined from the X-ray diagrams, are constant within the error of the measurement for the three V concentrations considered in this study (table 1).

The Mössbauer spectra were obtained at 5 K, 80 K and room temperature for non-oriented absorbers by using a conventional constant acceleration spectrometer. The source consisted of  $^{57}\text{Co}$  in Rh moving at room temperature while the absorber was kept fixed. Oriented absorbers of  $\text{NdFe}_{9.8}\text{V}_{2.2}$  alloy were prepared by mixing the powder sample with epoxy resin and letting it harden in an applied magnetic field of 1.6 T. The oriented samples were measured systematically at several temperatures in the range of 5–300 K.

Magnetic-moment measurements, as a function of temperature, were obtained for all samples in the range 5–700 K by using for low temperatures ( $T < 300$  K) a PAR-155 magnetometer and for high temperatures ( $320 \text{ K} < T < 700 \text{ K}$ ) a Perkin-Elmer thermogravimetric balance under the influence of a non-homogeneous weak magnetic field. Oriented samples were prepared in a similar manner as for Mössbauer absorbers.

## 3. Mössbauer results

The spectrum of a polycrystalline absorber of the  $\text{NdFe}_{9.8}\text{V}_{2.2}$  alloy at room temperature is shown in fig. 1. The most prominent feature of this spectrum is the differential broadening of the outer hyperfine lines relative to the center ones, due to different hyperfine parameters of the iron atoms occupying different crystallographic sites. A series

of spectra of an oriented absorber of the same compound in the temperature range of 5 to 228 K is shown in fig. 2. A marked increase of the intensity of the  $\Delta m = 0$  lines is observed as the temperature is lowered from 135 to 110 K. Since the experimental conditions of preparation of the absorbers were chosen so that the direction of gamma rays was parallel to the aligning field, this variation in intensity indicates a rotation of the easy axis of magnetization away from the direction of gamma rays. As already mentioned, the iron lattice anisotropy favors an easy axis of magnetization along the *c*-axis at room temperature. The above observation, therefore, is a manifesta-

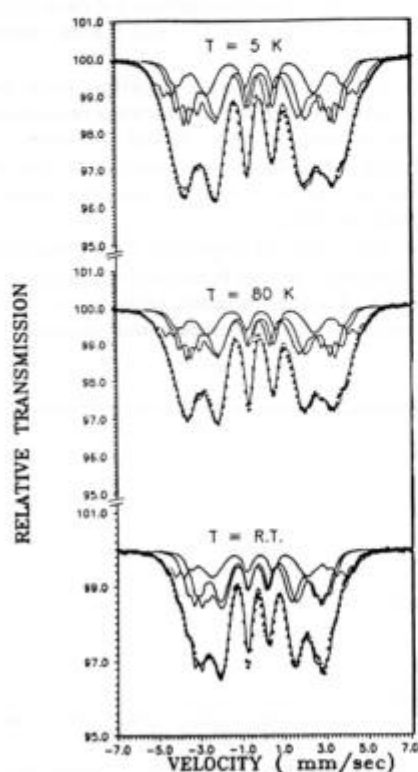


Fig. 1. Mössbauer spectrum of a polycrystalline absorber of  $\text{NdFe}_{9.8}\text{V}_{2.2}$  at three different temperatures.

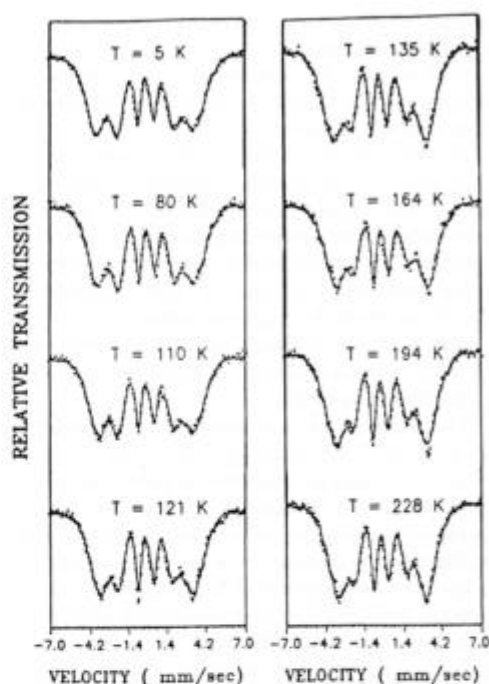


Fig. 2. Temperature dependence of Mössbauer spectra of an oriented absorber of  $\text{NdFe}_{9.8}\text{V}_{2.2}$ . The solid lines are computer fits using the model discussed in the text.

tion of spin reorientation as the temperature is lowered.

The iron (vanadium) atoms occupy three crystallographically different sites of the  $\text{ThMn}_{12}$  type structure, namely 8i, 8f and 8j. This means that, in the most favourable cases, one expects the  $^{57}\text{Fe}$  Mössbauer spectra of  $\text{NdFe}_{12-x}\text{V}_x$  compounds to consist of three different subspectra. In addition, the distribution of V atoms over the three 8i, 8f and 8j sites may split the subspectrum of each lattice site because of the statistical distribution around this site in different unit cells. As a result, for each crystallographic site we expect generally to have a subspectrum which is a sum of several components.

In order to solve the problem of polyparametrization in our analysis, we consider the following

restrictions based on a physically meaningful interpretation of the fit.

(i) For each site subspectrum we assume the same values for IS and QS for all the components from which it consists.

(ii) The effective field for the components of each subspectrum decreases linearly as the number of non-magnetic V neighbours increases, in accordance with Mössbauer studies of Fe-V alloys [10]. This assumption is supported also by the linear variation of  $T_C$  and  $M_s$  with V concentration found from the magnetic measurements.

(iii) The relative absorption of each component for every site subspectrum is calculated according to the following model:

The numbers of nearest-neighbour sites for 8i are (5, 4, 4, 1), for 8f are (4, 2, 4, 2) and for 8j are (4, 4, 2, 2) where the numbers in parentheses refer to 8i, 8f, 8j (Fe, V) and 2a (Nd) neighbours, respectively. According to neutron diffraction data [8] there is a preference of V atoms to occupy the 8i site. The examination of X-ray spectra does not give any evidence for the formation of superstructure. We supposed further that the probability  $p_i$  of finding a V atom at an 8i site is different and independent of the probability  $p_f$  and  $p_j$  of finding a V atom at a 8f or 8j site.

Assuming a binomial distribution of V atoms in the 8i, 8f and 8j sites we can readily calculate the probabilities of nearest neighbour configurations for a Fe atom in the 8i, 8f and 8j sites. Thus, the probability  $P_i(k)$  of an Fe atom in the 8i site to have  $k$  vanadium nearest neighbours is

$$P_i(k) = \sum P(n_i) \times P(n_f) \times P(n_j),$$

where  $P(n_i)$ ,  $P(n_f)$  and  $P(n_j)$  are the binomial distribution functions and  $n_i + n_f + n_j = k$  with  $k_{\max} = 13$ . The summation is over  $n_i$ ,  $n_f$  and  $n_j$ . A similar expression can be obtained for the probabilities  $P_f(k)$ ,  $P_j(k)$  of a configuration of  $k$  nearest V neighbours for an Fe atom in the 8f or 8j with  $k_{\max} = 10$ .

On the basis of these constraints the Mössbauer spectra were analyzed with a superposition of components corresponding to sites with specific configuration of nearest neighbours and relative intensities given by the associated probability.

Each component is a six-line spectrum with intensity ratios of  $3 : x : 1 : 1 : x : 3$  where  $x = 2$  in the case of non-oriented absorbers. It is used as a fitting parameter in oriented absorber spectra. The unit intensity proportional to the area of the spectrum is an additional parameter. Since only the components with  $k < 5$  have non-negligible probabilities, there are in total fifteen sextets (five for each site).

The sum of probabilities must satisfy the relation

$$4p_i + 4p_f + 4p_j = 2.2,$$

assuming that the nominal vanadium concentration is correct. The values deduced from the fit for all temperatures are  $p_i = 0.41$ ,  $p_f = 0.07$  and  $p_j = 0.07$ . From these results we may calculate the numbers of iron nearest neighbors for each site as 10.4, 7.9 and 7.9 for the i, j and f sites, respectively.

The values of the average hyperfine fields and isomer shifts for each site as functions of temperature are plotted in figs. 3 and 4. Values of quadrupole coupling are not given since they are found to be close to zero, within the error limits of the fitting procedure.

The assignment of hyperfine field parameters to the different sites has been made on the basis of the values of site occupation probabilities and a consideration of the number and distances of

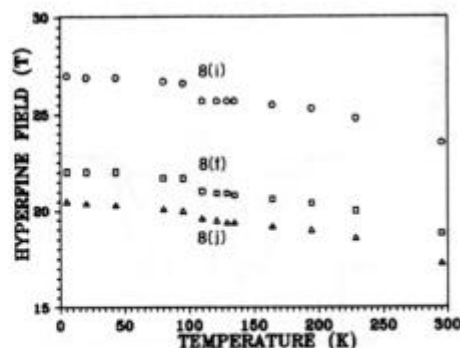


Fig. 3. Temperature dependence of the hyperfine field for the three iron sites i, f, j in the  $\text{ThMn}_{12}$  type structure of  $\text{NdFe}_{9.8}\text{V}_{2.2}$ .

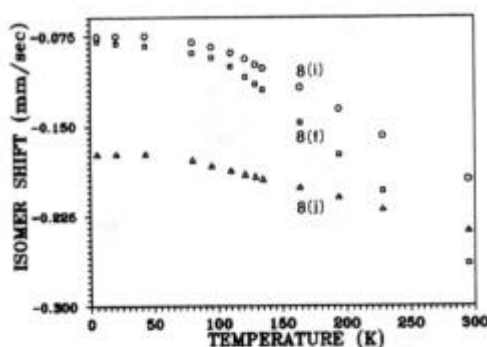


Fig. 4. Temperature dependence of the isomer shift for the three iron sites i, f, j in the  $\text{ThMn}_{12}$  type structure of  $\text{NdFe}_{9.8}\text{V}_{2.2}$ .

magnetic nearest neighbors. Specifically, the largest hyperfine field is assigned to the site which has the greatest number of iron neighbors (10.4) as determined above. The f and j sites, with the same number of iron neighbors are expected to have similar hyperfine fields, as is indeed found from the analysis. The larger of the two fields is assigned to the f-site on the basis of the slightly smaller average distance for the f-site. The data of fig. 3 show an abrupt change in the hyperfine field, most prominent for the i-site, between 100 and 110 K, which is indicative of the spin reorientation transition.

The variation of isomer shifts with temperature shows the expected decrease from the temperature dependence of the second-order Doppler shift. The assignment to crystallographic sites follows the assignment of hyperfine fields. The overall consistency of the fitting procedure is characterized by the use of the same occupation probabilities at all temperatures and the same hyperfine constants for fitting spectra of oriented and non-oriented absorbers at the same temperatures. Spectral lineshapes calculated with this procedure are shown as continuous lines in figs. 1 and 2.

#### 4. Magnetic measurements

The magnetization versus applied field was measured parallel to the alignment direction on

oriented samples of cylindrical shape at  $T = 5$  and 300 K up to a maximum field of 2 T. Values for the saturation magnetization  $M_s$  were derived from the high field part of isotherm curves by extrapolation with the law of approach to saturation [11], i.e.

$$M = M_s \left( 1 - \frac{b}{H^2} \dots \right).$$

Values of the Curie temperature  $T_C$  and saturation magnetization  $M_s$  of the studied alloys are given in table 1. These data show that, while the lattice constants do not change significantly with V concentration, we do have a linear variation of  $T_C$  which parallels the decrease of  $M_s$  with increasing  $x$ . This can be attributed to a variation of the exchange interaction with V concentration and is consistent with the assumed linear dependence of the hyperfine fields with the number of V nearest neighbors.

The measured variation of magnetization with temperature in a field of 50 mT for the alloy with  $x = 2.2$  is shown in fig. 5. Similar results have been obtained for the alloys with  $x = 1.8$  and  $x = 2$ . The sequence of the measurements was started at 4.2 K after an isothermal measurement up to 2 T. Values of the magnetization were then measured with increasing temperature up to room temperature and a new series of values was ob-

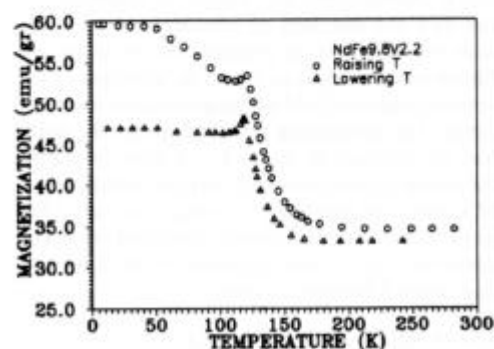


Fig. 5. Variation of magnetization with temperature for an oriented sample of  $\text{NdFe}_{9.8}\text{V}_{2.2}$ . The curve for ascending temperature has been obtained after an isotherm measurement up to 2 T at 5 K.

tained by lowering the temperature to 4.2 K. As shown in fig. 3, an abrupt change in the value of the magnetization occurs around 130 K, indicative of a transition in the magnetic structure, for both series measurements. A peak in magnetization is observed near 120 K just before the onset of the decrease in magnetization. The values obtained with increasing temperature are significantly greater than the corresponding values with decreasing temperature. This hysteretic behavior can be explained qualitatively by the variation in magnetic domains, as will be discussed below.

### 5. Analysis of Mössbauer and magnetic results

In order to deduce quantitatively the canting angle between the magnetization and the  $c$ -axis from the Mössbauer and magnetization data presented above, we have used and extended the methods presented in previous investigations of similar problems [2,6]. We assume that the oriented absorbers consist of assemblies of monocrystalline grains with a distribution function along the direction of the  $c$ -axis given by the expression

$$P(\theta) = (n+1) \cos^n \theta, \quad n > 0, \quad (1)$$

where  $\theta$  is the angle between the  $c$ -axis and the direction of measurement and  $n$  is a parameter which characterizes the degree of alignment. In our case the direction of measurement coincides with the direction of propagation of  $\gamma$ -rays for Mössbauer absorbers and with the direction of the applied magnetic field for magnetization measurements. The geometrical relationships for the problem are depicted in fig. 6. For a given crystallite the magnetization may lie anywhere on the surface of a cone with half angle  $\alpha$  around the  $c$ -axis. The angle  $\psi$  between the magnetization and the  $z$ -axis determines the relative intensity of the  $\Delta m = \pm 1$  and  $\Delta m = 0$  Mössbauer lines

$$I_1 = (3/2)[1 + \cos^2 \psi(\alpha, \theta, \varphi')],$$

$$I_2 = 2 \sin^2 \psi(\alpha, \theta, \varphi').$$

For comparison with experimental results an

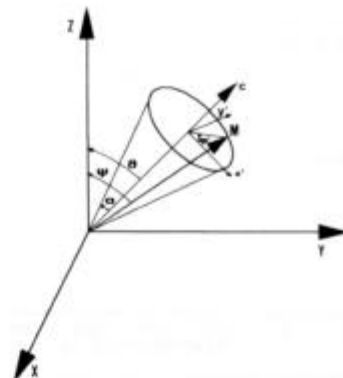


Fig. 6. Angular relations of the orientation axis, the  $c$ -axis and the direction of magnetization used in the calculations.

appropriate average must be taken over the angles  $\varphi'$  of  $\theta$ . This has been calculated by Hu et al. [2]

$$\langle I_1 \rangle = \frac{3}{2} \left[ 1 + \left( \frac{n+1}{n+3} \right) \cos^2 \alpha + \left( \frac{1}{n+3} \right) \sin^2 \alpha \right], \quad (2)$$

$$\langle I_2 \rangle = 2 \left[ 1 - \left( \frac{n+1}{n+3} \right) \cos^2 \alpha - \left( \frac{1}{n+3} \right) \sin^2 \alpha \right]. \quad (3)$$

It is convenient to express the results in terms of an average angle  $\psi_{av}(\alpha)$  defined by

$$\langle I_1 \rangle = \frac{3}{2} [1 + \cos^2 \psi_{av}(\alpha)], \quad (4)$$

$$\langle I_2 \rangle = 2 \sin^2 \psi_{av}(\alpha). \quad (5)$$

Then

$$\sin \psi_{av}(\alpha) = \sqrt{2} \left[ \frac{4}{3} R(\alpha) + 1 \right]^{-1/2}, \quad (6)$$

where  $R(\alpha) = \langle I_1 \rangle / \langle I_2 \rangle$ . When the magnetic moments lie along the  $c$ -axis ( $\alpha = 0$ ) the intensity ratio found from eqs. (2) and (3) is

$$R(0) = \frac{3}{2}(n+2), \quad (7)$$

Then using eq. (6)

$$n = 2 \tan^{-2} \psi_0 - 1, \quad \text{where } \psi_0 = \psi_{av}(0). \quad (8)$$

It is known that the magnetic moments lie along the  $c$ -axis at room temperature. Using the corresponding intensity ratio from table 2 we find

Table 2

Ratio of average intensities  $\langle I_1 \rangle / \langle I_2 \rangle$  of the relative absorption parameters from  $\Delta m = 0$  transitions fitted from Mössbauer spectra and the canting angle  $\alpha$  as a function of temperature

$T$ (K)	$\langle I_1 \rangle / \langle I_2 \rangle$	$\alpha$ (°)
295	2.31	0.0
228	2.31	0.0
194	2.31	0.0
164	2.31	0.0
135	2.14	15.0
129	2.04	22.0
121	1.92	30.0
110	1.72	42.0
95	1.62	47.0
80	1.58	49.0
43	1.58	49.0
20	1.58	49.0
5	1.58	49.0

$\psi_0 = 45^\circ$  and  $n = 1$ . With  $\psi_0$  as a parameter we find for the canting angle

$$\sin^2 \alpha = \frac{\sin^2 \psi_{av}(\alpha) - \sin^2 \psi_0}{1 - \frac{1}{2} \sin^2 \psi_0}, \quad (9)$$

with  $\psi_{av}(\alpha)$  determined from the experimental results by using eq. (6). The canting angles determined by this procedure are listed in table 3 and plotted in fig. 7. We observe that the rotation of the moments from the  $c$ -axis starts at 160 K and is completed at 90 K with an abrupt change in the interval 129–110 K.

The variation of the canting angle with temperature can be determined also by an analysis of the thermomagnetic curves. Following previous investigations for similar systems [6,12], the average of the normalized projection of the magnetic moment of individual particles along the direction of the applied field is

$$\begin{aligned} M/M_0 &= \overline{\cos \psi(h)} \\ &= \int_0^{\pi/2} \cos \psi(h) P(\theta) \sin \theta d\theta, \end{aligned} \quad (10)$$

where  $P(\theta)$  is the normalized distribution function of the orientation of crystallites and the angles  $\theta$  and  $\psi$  are as defined in fig. 6. The argument  $h$  indicates a possible dependence of  $\psi$  on the applied field.

Table 3

Magnetization measurements and calculated values of the canting angle  $\alpha$  from thermomagnetic measurements as a function of temperature

$T$ (K)	$M$ ( $\text{Am}^2 \text{ kg}^{-1}$ )	$\alpha$ (°)
290	33.2	0.0
242	33.2	0.0
208	33.2	0.0
180	33.2	0.0
165	33.4	0.4
155	33.9	1.3
141	36.0	5.0
136	37.4	7.9
128	40.9	15.7
125	43.4	22.5
122	45.3	30.8
112	46.7	39.6
110	46.9	43.9
102	46.9	43.9
82	46.9	43.9
51	46.9	43.9
31	46.9	43.9
12	46.9	43.9

In the case where the magnetization lies along the easy axis (high temperatures),  $\psi = \theta$  since the applied field (50 mT) is much smaller than the anisotropy field and cannot rotate the magnetization away from the easy axis. With this assumption, eq. (10) gives

$$M/M_0 = \overline{\cos \psi} = \overline{\cos \theta} = (n+1)/(n+2). \quad (11)$$

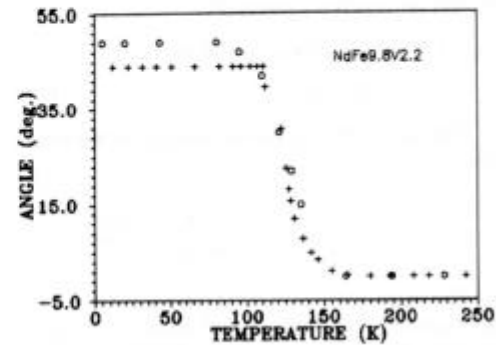


Fig. 7. Canting angle as a function of temperature for  $\text{NdFe}_{9.8}\text{V}_{2.2}$  determined from Mössbauer ( $\circ$ ) and magnetization (+) data.



With the value of  $n=1$  estimated from the Mössbauer results, we get  $M_0 = \frac{2}{3}M$ . Using the room temperature result we find  $M = \frac{3}{2}33.2 = 49.8 \text{ Am}^2 \text{ kg}^{-1}$ .

In the case of easy cone, since all directions on the surface of the cone are energetically equivalent, the application of a magnetic field results in a rotation of the magnetization to the nearest angle to the  $z$ -axis. In that case  $\psi(h) = \theta - \alpha$ , and eq. (10) gives

$$M/M_0 = \overline{\cos(\theta - \alpha)} = \frac{2}{3}[\cos \alpha + \sin \alpha] \text{ for } n=1. \quad (12)$$

From the condition  $d \overline{\cos(\theta - \alpha)} / d\alpha = 0$  we find the value of  $\alpha$  for which the ratio  $M/M_0$  reaches its maximum value, i.e.

$$\tan \alpha = 1 \quad \text{and} \quad \alpha = 45^\circ,$$

which corresponds to a maximum value of  $M = 0.94M_0$ . This result, of course is specific to the orientation distribution prevailing in our sample.

The angle  $\alpha$ , as a function of temperature, can be obtained by solving eq. (12) for different values of  $M/M_0$  measured at different temperatures. Substituting

$$\sin \alpha = \frac{2 \tan(\alpha/2)}{1 + \tan^2(\alpha/2)} \quad \text{and}$$

$$\cos \alpha = \frac{1 - \tan^2(\alpha/2)}{1 + \tan^2(\alpha/2)},$$

we get the quadratic equation

$$\left[ \frac{2}{3} + (M/M_0) \right] \tan^2(\alpha/2) - \frac{4}{3} \tan(\alpha/2) - \frac{2}{3} + M/M_0 = 0. \quad (13)$$

The physically acceptable solution of this equation is

$$\alpha = 2 \tan^{-1} \frac{\frac{4}{3} - \left\{ \frac{16}{9} - 4 \left[ (M/M_0)^2 - \frac{4}{9} \right] \right\}^{1/2}}{2 \left( \frac{2}{3} + M/M_0 \right)}.$$

The values of  $\alpha$  calculated from this expression are tabulated in table 3 and plotted in fig. 7, together with the results of the Mössbauer analysis. We have used in this tabulation the values of  $M$  obtained with decreasing temperature since, as

will be discussed below, they conform better to the approximation used in this model.

The agreement is fairly good, especially with regard to the variation of the angle in the spin reorientation range.

## 6. Discussion

In the foregoing sections we have determined the temperature variation of the canting angle of the magnetization with respect to the  $c$ -axis for the compound  $\text{NdFe}_{9.8}\text{V}_{2.2}$  by two different methods, namely the variation of Mössbauer spectra and magnetic moment with temperature in oriented samples. The distribution of orientation of crystallites within the sample was taken explicitly into account. We shall examine now some of the most important assumptions and approximations underlying this analysis.

The principal implicit assumption is that both the oriented Mössbauer absorbers and the cylindrically shaped oriented samples used in the magnetic measurements consist of single domain crystallites with their  $c$ -axes statistically distributed with preferential orientation around the direction of measurement (the direction of the gamma rays in Mössbauer measurements and of the applied field in magnetic measurements). This means that each particle possesses the same saturation magnetization  $M_0$ . This is a rough approximation. Actually,  $M_0$  in the calculation represents an average spontaneous magnetization for a multidomain crystallite. At room temperature we have estimated previously  $M_0 = 49.8 \text{ Am}^2 \text{ kg}^{-1}$ , which is about half the saturation magnetization determined from high-field measurements. The Mössbauer results are not affected by this approximation since they depend on the aligned atomic magnetic moments. In view of the fairly good agreement of the angles calculated by the two methods we may conclude that the approximation that we have used does not seriously affect the results.

There are two features of the magnetization data which are not reproduced in the calculation. The first is the peak observed in the spin reorientation range and the second is the different behav-



ior with ascending and descending temperature. The first effect can be qualitatively explained by the rearrangement of domains near the spin reorientation temperature as a result of the variation of the magnetocrystalline anisotropy energy constants  $K_1$  and  $K_2$  with temperature. It is well known that the sizes of domain walls depend on the counterbalance of wall energy, magnetostatic energy and elastic energy. The domain-wall energy, which depends on the crystallographic orientation of the wall is proportional to  $(AK_1)^{1/2}$  to a first approximation [11], where  $A$  is a coefficient related to the exchange energy and  $K_1$  is the sum of  $K_1(\text{R})$  and  $K_1(\text{Fe})$  from the Nd and Fe sublattices. Since the anisotropy constants of the two sublattices are of opposite sign, we expect the total anisotropy constant to vary continuously with temperature, pass from zero and change sign in order to alter the easy axis of magnetization. A change of the domain wall pattern may occur during this process and the enhanced domain wall mobility may account for the observed peak in the magnetization, as has already been observed in  $\text{RCo}_5$  alloys [15].

A similar qualitative explanation may be given for the difference in magnetization with ascending and descending temperature. The measurements have been obtained first with ascending temperature with an oriented sample after isotherm measurements at 5 K. Hence, the resulting distribution of domain magnetization at the remanence point is different than that obtained when the sample is cooled from room temperature in a small field and gives higher average magnetization per crystallite. When the temperature is raised, the thermal agitation together with the spin reorientation erase the effect of the application of the field of 2 T and cause a drop in the measured magnetic moment as indeed is observed in the upper curve of fig. 5. It is worth noting that the peak in magnetization is not observed in non-oriented samples [3], presumably due to the random distribution of the easy axis direction in these samples. We note also that both the magnetization and the Mössbauer results indicate that the spin reorientation does not involve a complete rotation by  $\pi/2$  as in other compounds of this group, e.g.  $\text{DyFe}_{11}\text{Ti}$  [5]. Similar measurements in these compounds would show

a drop in magnetization at low temperatures, as is indeed observed, in agreement with eq. (12) which for  $\alpha = \pi/2$  gives  $M/M_0 = \frac{2}{3}$ . In our case, with a limiting value of  $\alpha = 45^\circ$ , the magnetization retains its maximum value at low temperatures.

The Mössbauer results exhibit also the spin reorientation by an abrupt change of the hyperfine field of the three different sites, which is most pronounced for the i-site. Franse et al. have argued recently [13] that the change in hyperfine field is directly related to the anisotropy energy of the individual sites and is proportional to the anisotropy energy constant. The results given in fig. 3 would then imply a considerably higher anisotropy energy for the i-site.

The fitting of Mössbauer lineshapes by means of a model which assumes different probabilities of occupation for the i, j and f sites has confirmed the preferential occupation of the i site by V. In the range of concentrations studied, the V concentration does not seem to affect the spin reorientation temperature and the temperature range of the transition. These parameters, however, are different for the  $\text{NdFe}_{9.9}\text{Mo}_{2.2}$  [14] and  $\text{NdFe}_{11}\text{Ti}$  [1] compounds. Since the crystal structure and the rare earth ion remain the same we expect that the crystal-field parameters for the Nd ion will be the same in the three compounds. We may conclude that the additive transition element T in the compounds  $\text{NdFe}_{12-x}\text{T}_x$  affects the spin reorientation transition mainly by altering the crystal-field anisotropy of the iron sublattice. As shown in previous investigations [1,5], the crystal-field parameters can be determined from the temperature dependence of the canting angle. Similar calculations for the compounds studied in this work are in progress and will be reported elsewhere.

## 7. Conclusion

The occurrence of a spin reorientation transition has been detected in the ternary  $\text{NdFe}_{12-x}\text{V}_x$  compounds ( $x = 1.8, 2.0, 2.2$ ) by measurements on oriented samples of (a) the temperature dependence of the relative intensity of Mössbauer lines and (b) the variation of magnetization with tem-

perature. The temperature dependence of the canting angle was determined from the results of both methods and was found to be in fair agreement.

The model used for the calculation has included a distribution of orientations of the  $c$ -axis of the compounds around the direction of the orienting field. It has been found that the magnetic moment rotates from a direction along the  $c$ -axis at room temperature to an angle of  $45^\circ$  with respect to this axis at low temperature. The spin reorientation transition does not depend on the V content and occurs at 130 K within a range of approximately 30 K.

The Mössbauer results have verified the preferential occupation of the i sites by V in the  $\text{ThMn}_{12}$  type structure. The methodology established for the analysis of Mössbauer spectra, as well as for the magnetization measurements, may be generally applicable in spin reorientation studies.

#### Acknowledgement

This work has been supported in part by a EURAM/BRITE Grant from the European Economic Communities.

#### References

- [1] Hu Bo-Ping, Li Hong-Shuo, J.P. Gavigan and J.M.D. Coey, *J. Phys. Condens. Matter* 1 (1989) 755.
- [2] Hu Bo-Ping, Li Hong-Shuo and J.M.D. Coey, *Hyperfine Interactions* 45 (1989) 233.
- [3] C. Christides, A. Kostikas, D. Niarchos and A. Simopoulos, *J. de Phys.* 49 (1988) C8-539.
- [4] F.R. De Boer, Ying-Kay Huang, D.B. De Mooij and K.H.J. Buschow, *J. Less-Common Met.* 135 (1987) 199.
- [5] Li Hong-Shuo, Hu Bo-Ping and J.M.D. Coey, *Solid State Commun.* 66 (1988) 133.
- [6] C.W. Searle, V. Davis and R.D. Hutchens, *J. Appl. Phys.* 53 (1982) 2395.
- [7] G. Zouganelis, A. Kostikas, A. Simopoulos and D. Niarchos, *J. Magn. Magn. Mat.* 75 (1988) 91.
- [8] R.B. Helmholdt, J.J.M. Vleggar and K.H.J. Buschow, *J. Less-Common Met.* 138 (1988) L11.
- [9] K.H.J. Buschow and D.B. De Mooij, CEAM Final Report (1989) (Commission of the European Communities) p. 63.
- [10] N.K. Jaggi, L.H. Schwartz, H.K. Wong and J.B. Ketterson, *J. Magn. Magn. Mat.* 49 (1985) 1.
- [11] S. Chikazumi, *Physics of Magnetism* (John Wiley, New York, 1964).
- [12] R.W. Chantrelli, B.K. Tanner and S.R. Itoon, *J. Magn. Magn. Mat.* 38 (1983) 83.
- [13] J.J.M. Franse, N.P. Thuy and N.M. Hong, *J. Magn. Magn. Mat.* 72 (1988) 361.
- [14] Christides et al., unpublished.
- [15] H.R. Kirchmayer and C.A. Poldy, *Handbook on the Physics and Chemistry of Rare Earths*, vol. 2, eds. K.A. Gschneidner and L. Eyring (North-Holland, Amsterdam, 1979) chap. 14, p. 161.